

Research Article

A Comparison of Finite Difference and Finite Volume Methods with Numerical Simulations: Burgers Equation Model

Ali Hasan Ali ^{1,2}, Ahmed Shawki Jaber,³ Mustafa T. Yaseen,⁴ Mohammed Rasheed,⁵ Omer Bazighifan ^{6,7} and Taher A. Nofal⁸

¹Department of Mathematics, College of Education for Pure Sciences, University of Basrah, Basrah, Iraq

²Doctoral School of Mathematical and Computational Sciences, University of Debrecen, H-4002 Debrecen, Pf 400, Hungary

³Department of Mechanical and Materials Engineering, Wright State University, 3640 Colonel Glenn Hwy, Dayton, OH 45435, USA

⁴Department of Business Administration, Shatt Al-Arab University College, Basrah, Iraq

⁵Applied Sciences Department, University of Technology, Baghdad, Iraq

⁶Department of Mathematics, Faculty of Science, Hadhramout University, Hadhramout 50512, Yemen

⁷Department of Mathematics, Faculty of Education, Seiyun University, Hadhramout 50512, Yemen

⁸Department of Mathematic, College of Science, Taif University, P.O Box 11099, Taif 21944, Saudi Arabia

Correspondence should be addressed to Omer Bazighifan; o.bazighifan@gmail.com

Received 5 May 2022; Accepted 1 June 2022; Published 27 June 2022

Academic Editor: Fathalla A. Rihan

Copyright © 2022 Ali Hasan Ali et al. This is an open access article distributed under the Creative Commons Attribution License, which permits unrestricted use, distribution, and reproduction in any medium, provided the original work is properly cited.

In this paper, we present an intensive investigation of the finite volume method (FVM) compared to the finite difference methods (FDMs). In order to show the main difference in the way of approaching the solution, we take the Burgers equation and the Buckley–Leverett equation as examples to simulate the previously mentioned methods. On the one hand, we simulate the results of the finite difference methods using the schemes of Lax–Friedrichs and Lax–Wendroff. On the other hand, we apply Godunov’s scheme to simulate the results of the finite volume method. Moreover, we show how starting with a variational formulation of the problem, the finite element technique provides piecewise formulations of functions defined by a collection of grid data points, while the finite difference technique begins with a differential formulation of the problem and continues to discretize the derivatives. Finally, some graphical and numerical comparisons are provided to illustrate and corroborate the differences between these two main methods.

1. Introduction

In finite difference methods (FDMs), the differential equation is approximated by a set of algebraic equations (see [1, 11, 12]). These approximations are usually improved with the use of more terms and the use of smaller grid spacing (also known as more nodes). Starting with a variational formulation of the problem, the finite element technique provides piecewise formulations of functions defined by a collection of grid data points. The finite difference technique begins with a differential formulation of the problem and continues to discretize the derivatives [15]. Like any approximation, finite difference schemes have their limitations such as oscillations and diffusion especially at points of

discontinuity. Another issue that FDM runs into is that mass is only conserved when the grid spacing goes to zero and they struggle with irregular geometry [2, 10]. Usually, a FDM’s grid looks like the following (Figure 1).

However, in some geometries, it may not be possible to align the grid with perpendicular grid lines which means one might not be able to approximate some derivatives in terms of the values along a constant “*i*” line. Because of these shortcomings, some have turned to using control volume formulation or finite volume methods (FVMs). This started back in 1960 when it was called the integration method, and it turned out to have many applications in oscillation theory and diffusive convection [4–8]. Most recently, FVMs have been used in computational fluid dynamics because of their

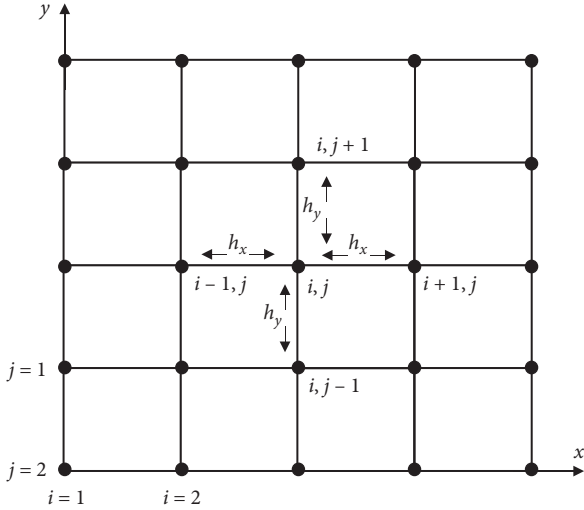


FIGURE 1: An FDM's grid.

ability to be used on unstructured meshes [3]. In general, in the FVM, the differential equation is integrated over a control volume and then discretized using some approximations. Another aspect of the huge advantages of using the FVM is that material (like mass or energy) is conserved because it uses integration over small volumes, and since the flux, which is the flow of material in space with time, of the material at the common side is represented by the same expression, this implies that global conservation is also ensured. In fact, both FDM and FVM have a huge number of applications in many engineering and natural science fields. Several important applications of the FDM can be found in computer vision, image processing, solving diffusion convection, and thermal problems (see [9, 13, 14]). On the other hand, the applications of FVM appear in many fields, and its software can be used in several branches, such as solid mechanics, thermal and electrical analysis, structural analysis, oscillation theory, and mechanical engineering design (see [16–21]). The structure of this paper is organized as follows. In Section 2, we provide the definition and the mechanism of the finite volume method (FVM). In Section 3, we consider a one-dimensional application of the FVM. In Section 4, we use an inviscid Burgers equation to apply the proposed comparison of the mentioned numerical methods. Finally, several simulations for the Burgers equation and one simulation for the Buckley–Leverett equation with the main results are presented in Section 5.

2. Finite Volume Method (FVM)

To understand the finite volume method, we need to start with the conservation form of the transport equation, which is given as

$$\frac{\partial T}{\partial t} + \nabla \cdot (\vec{u}T) = \nabla \cdot (\alpha \nabla T). \quad (1)$$

This partial differential equation is used on the infinitesimal volumes described in Figure 2.

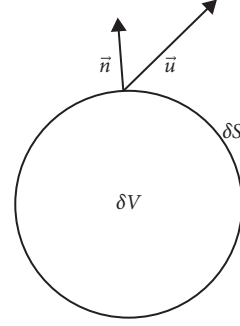


FIGURE 2: A PDE on an infinitesimal volume.

Knowing that the infinitesimal discrete volumes are unaffordable, they would need to be of some larger finite size. Now we derive the conservation form for a finite volume δV bounded by a surface, which we will denote as δS . Applying the integral gives us the following:

$$\int_{\delta V} \frac{\partial T}{\partial t} dV + \int_{\delta V} \nabla \cdot (\vec{u}T) dV = \int_{\delta V} \nabla \cdot (\alpha \nabla T) dV. \quad (2)$$

If we assume the volume to be fixed in space, we can interchange the order of integration in space and differentiation in time:

$$\frac{d}{dt} \left(\int_{\delta V} T dV \right) + \int_{\delta V} \nabla \cdot (\vec{u}T) dV = \int_{\delta V} \nabla \cdot (\alpha \nabla T) dV. \quad (3)$$

The understanding of the first integral on the left is the time rate of change of the T inside volume δV . The Gauss divergence theorem is necessary for the next step. The theorem says that the outward flux of a vector field through some closed surface is equal to the volume integral of the divergence over the region inside the surface. So, basically, we are going to change our equation from volume integrals to surface integrals.

$$\frac{d}{dt} \left(\int_{\delta V} T dV \right) + \int_{\delta S} \vec{n} \cdot \vec{u}T dV = \int_{\delta S} \vec{n} \cdot \alpha \nabla T dV, \quad (4)$$

where \vec{n} represents the outward part that is normal to the surface. The surface integral on the left describes the “in and out” advection flux across the surface of the volume. The one on the other side describes the diffusive transport of T across the surface. The equation can be summarized as the rate of change of the T value in δV which is equal to the rate of transport T through the surface by advection and diffusive fluxes. Notice that we have not given the surface a definite size or shape, so this equation could be applied to whatever we would like. Note the order of the derivatives as they appear in the differential equation (1) versus those of the integral form (4). In the differential equation, we have a first-order advection term and a second-order diffusion term, but in the integral form, there is a 0-th order advection term and a first-order diffusion term. This is an important change because it helps with problems that have discontinuities of the spatial derivative. Examples of those types are the problems that have shock or hydraulic jump.

Now we introduce the average T in δV which we will refer to as

$$\bar{T} = \frac{1}{\delta V} \int_{\delta V} T dV. \quad (5)$$

The integral conservation law can now be written as a time evolution equation:

$$\delta V \frac{d\bar{T}}{dt} + \int_{\delta S} \vec{n} \cdot \vec{u} T dV = \int_{\delta S} \vec{n} \cdot \alpha \nabla T dV. \quad (6)$$

It is important to note that equations (4) and (6) are exact solutions and no approximation has yet been introduced. The approximation will come from

- (1) Temporal integration of the equations.
- (2) Calculation of the fluxes in space and time.

However, the first step is to divide the domain into a discrete number of cells which we will denote as δV_j where the cell average is known. After that, we calculate the advection and diffusion fluxes through function reconstruction, followed by evaluation of the integrals, and finally the temporal integration with a forward marching time step.

3. Application of the FVM

We consider here only the 1-D case. Therefore, we first break up the domain as shown in Figure 3.

The cell centres are denoted by the integer numbers and the cell edges are denoted by the fractions. In this case, the cells are line segments, and the cell ‘‘volumes’’ are reduced to just cell widths δx (which we will assume as uniform throughout). This means that the flux integrals reduce to the evaluation of the term at the cell edges, which means the conservation law can be rewritten as

$$\frac{d\bar{T}_j}{dt} = -\frac{F_{j+(1/2)} - F_{j-(1/2)}}{\delta x} + \frac{D_{j+(1/2)} - D_{j-(1/2)}}{\delta x}, \quad (7)$$

where F is the advection flux and D is the diffusive flux at the cell edge $x_{j+(1/2)}$.

The other assumption that we will make is that we are using a piecewise constant approximation as shown in Figure 4.

This means that we have the following approximation:
 $T = a_0$.

We can now write

$$\int_{x_{j-(1/2)}}^{x_{j+(1/2)}} a_0 dx = \delta x_j \bar{T}_j, \quad (8)$$

because we only have one unknown coefficient. Basically, the integral of T over a cell gives us $\delta x_j \bar{T}_j$. This means that the solution is $a_0 = \bar{T}_j$, which finishes our function reconstruction. Note that at each cell edge, there are two different values. For the advection term, we should use the upstream edge (what goes into the next term has to come from the previous term). This leads to

$$T_{j+(1/2)} = \begin{cases} \bar{T}_j, & u_{j+(1/2)} \geq 0, \\ \bar{T}_{j+1}, & u_{j+(1/2)} < 0. \end{cases} \quad (9)$$

The other implication of this is that piecewise constant functions cannot be used to compute the diffusive term because they have a zero derivative in space. This will not pose a problem for us later because we will be considering Burgers and the Buckley–Leverett equations which do not have a diffusive term.

4. Numerical Methods

Take a look at the inviscid Burgers equation

$$u_t + u \cdot u_x = 0. \quad (10)$$

Applying the Euler forward in time and backward in space discretization, one would come up with

$$U_j^{n+1} = U_j^n - \frac{k}{h} U_j^n (U_j^n - U_{j-1}^n). \quad (11)$$

This is sometimes referred to as the nonconservative upwind scheme. This method works well on nice smooth solutions but will not converge at discontinuous points as the grid is refined (see Figure 5).

To avoid this issue, we apply the conservation form

$$U_j^{n+1} = U_j^n - \frac{k}{h} [F(U_{j-p}^n, U_{j-p+1}^n, \dots, U_{j+q}^n) - F(U_{j-p-1}^n, U_{j-p}^n, \dots, U_{j+q-1}^n)], \quad (12)$$

where F is the numerical flux function. In general, methods that follow this type of scheme are called conservative methods. So, all the methods to follow were implemented using this type of scheme.

For the comparisons, we used the general conservation law:

$$u_t + [f(u)]_x = 0, \quad (13)$$

where for the Burgers equation, we use

$$f(u) = \frac{1}{2} u^2, \quad (14)$$

and for the Buckley–Leverett equation, we use

$$f(u) = \frac{u^2}{u^2 + 1/4(1-u)^2}. \quad (15)$$

The basic setup for the two different kinds of methods is as follows.

4.1. Finite Difference Methods

- (1) Set up grid (or nodes).

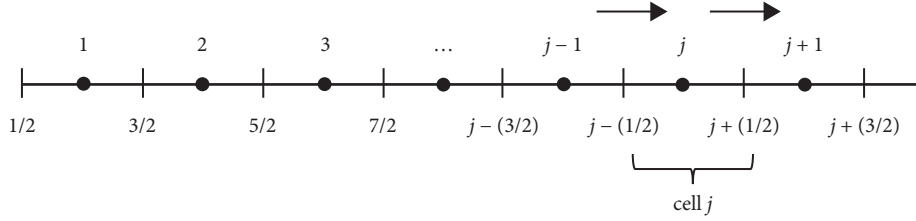


FIGURE 3: A sample domain of a 1-D case.

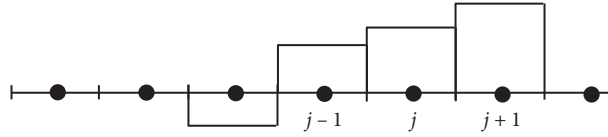


FIGURE 4: A piecewise constant approximation.

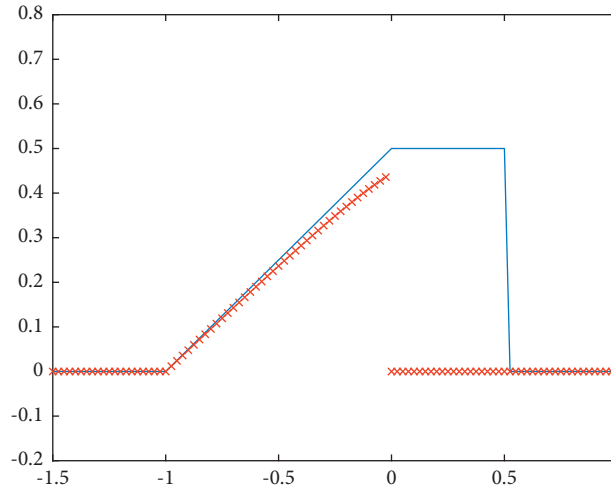


FIGURE 5: A nonconservative upwind method.

- (2) Approximate and replace all the derivatives by their corresponding finite difference approximations.
- (3) Solve the resulting algebraic system of equations.

4.2. Finite Volume Methods

- (1) Grid generation.
- (2) Discretize the integral conservation equation on control volumes.
- (3) Solve the resultant discrete integral/flux equations.

4.3. *Upwind Conservative Method.* In fact, this method is first-order accurate in both time and space; however, it is

only stable in the interval $0 \leq a(k/h) \leq 1$, where k is the size of the time step and h is the size of the space step.

Then, applying the standard finite difference upwind definition, we would get

$$U_j^{n+1} = U_j^n - \frac{k}{h} [f(U_j^n) - f(U_{j-1}^n)]. \quad (16)$$

Then, applying this to the Burgers equation, we get

$$U_j^{n+1} = U_j^n - \frac{k}{h} \left[\frac{1}{2}(U_j^n)^2 - \frac{1}{2}(U_{j-1}^n)^2 \right]. \quad (17)$$

Moreover, we apply this method to the Buckley–Leverett equations to get

$$U_j^{n+1} = U_j^n - \frac{k}{h} \left[\frac{(U_j^n)^2}{(U_j^n)^2 + 1/4(1 - U_j^n)^2} - \frac{(U_{j-1}^n)^2}{(U_{j-1}^n)^2 + 1/4(1 - U_{j-1}^n)^2} \right]. \quad (18)$$

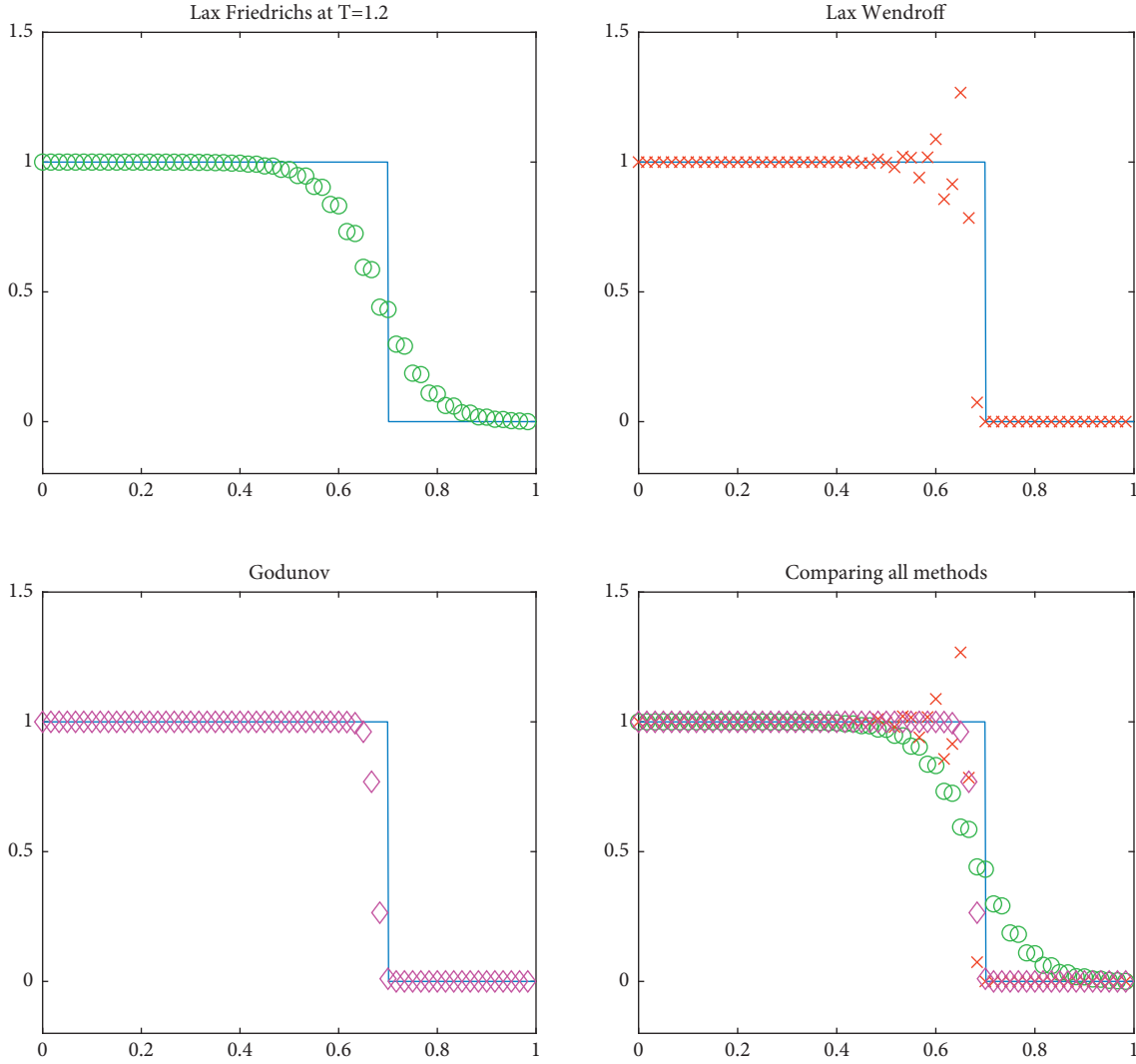


FIGURE 6: Graphs for the single shock simulation.

4.4. Lax–Friedrichs Method. Like the upwind conservative method, the Lax–Friedrichs method is first-order accurate in time and space. In addition, it has a stability requirement of $|ak/h| \leq 1$. The Lax–Friedrichs method takes the form

$$U_j^{n+1} = \frac{1}{2}(U_{j-1}^n + U_{j+1}^n) - \frac{k}{2h} [f(U_{j+1}^n) - f(U_{j-1}^n)]. \quad (19)$$

Then, applying this to the Burgers equation, we get

$$U_j^{n+1} = \frac{1}{2}(U_{j-1}^n + U_{j+1}^n) - \frac{k}{h} \left[\frac{1}{2}(U_{j+1}^n)^2 - \frac{1}{2}(U_{j-1}^n)^2 \right]. \quad (20)$$

For the Buckley–Leverett equation, we would have

$$U_j^{n+1} = \frac{1}{2}(U_{j-1}^n + U_{j+1}^n) - \frac{k}{2h} \left[\frac{(U_{j+1}^n)^2}{(U_{j+1}^n)^2 + 1/4(1 - U_{j+1}^n)^2} - \frac{(U_{j-1}^n)^2}{(U_{j-1}^n)^2 + 1/4(1 - U_{j-1}^n)^2} \right]. \quad (21)$$

4.5. Lax–Wendroff Method. The Lax–Wendroff method is second-order accurate in both time and space, and it has a known stability of $|ak/h| \leq 1$. For the nonlinear conservation laws, it takes the form

$$U_j^{n+1} = U_{j+1}^n - \frac{k}{2h} (f(U_{j+1}^n) - f(U_{j-1}^n)) + \frac{k^2}{2h^2} [A_{j+1/2}(f(U_{j+1}^n) - f(U_j^n)) - A_{j-1/2}(f(U_j^n) - f(U_{j-1}^n))]. \quad (22)$$

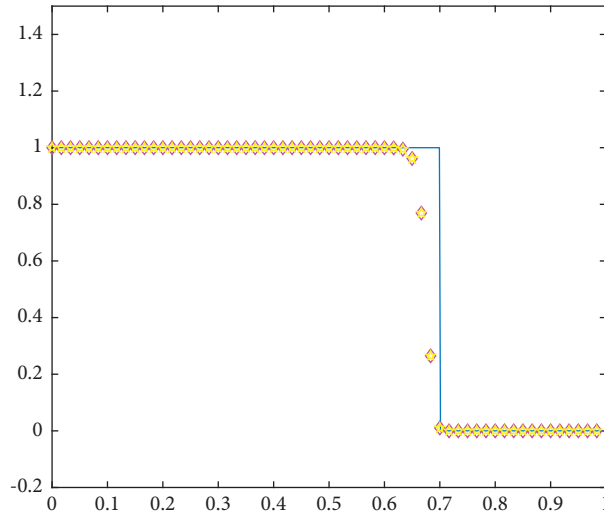


FIGURE 7: Comparing the Godunov method to the upwind method.

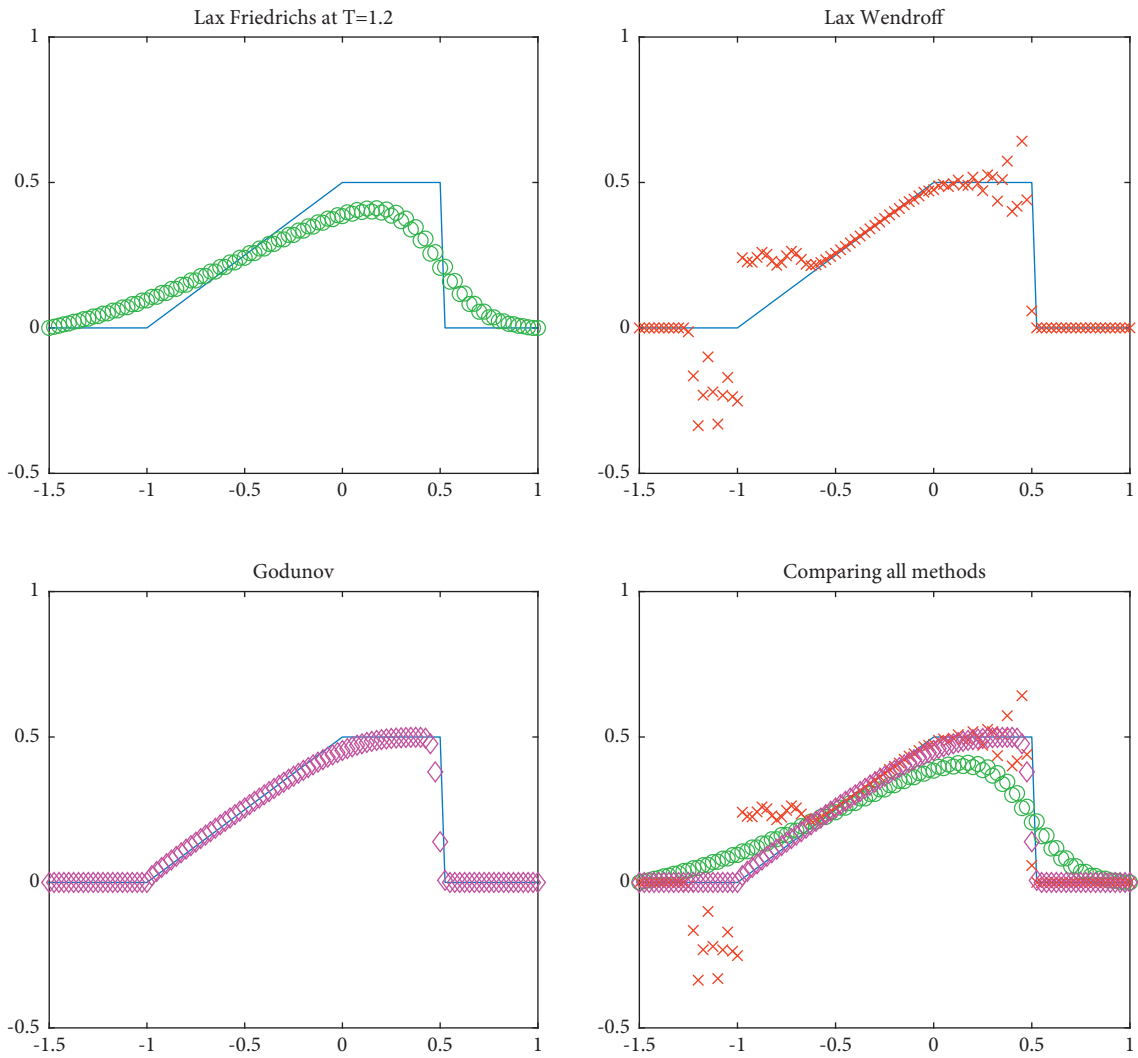


FIGURE 8: Graphs for the traveling pulse simulation.

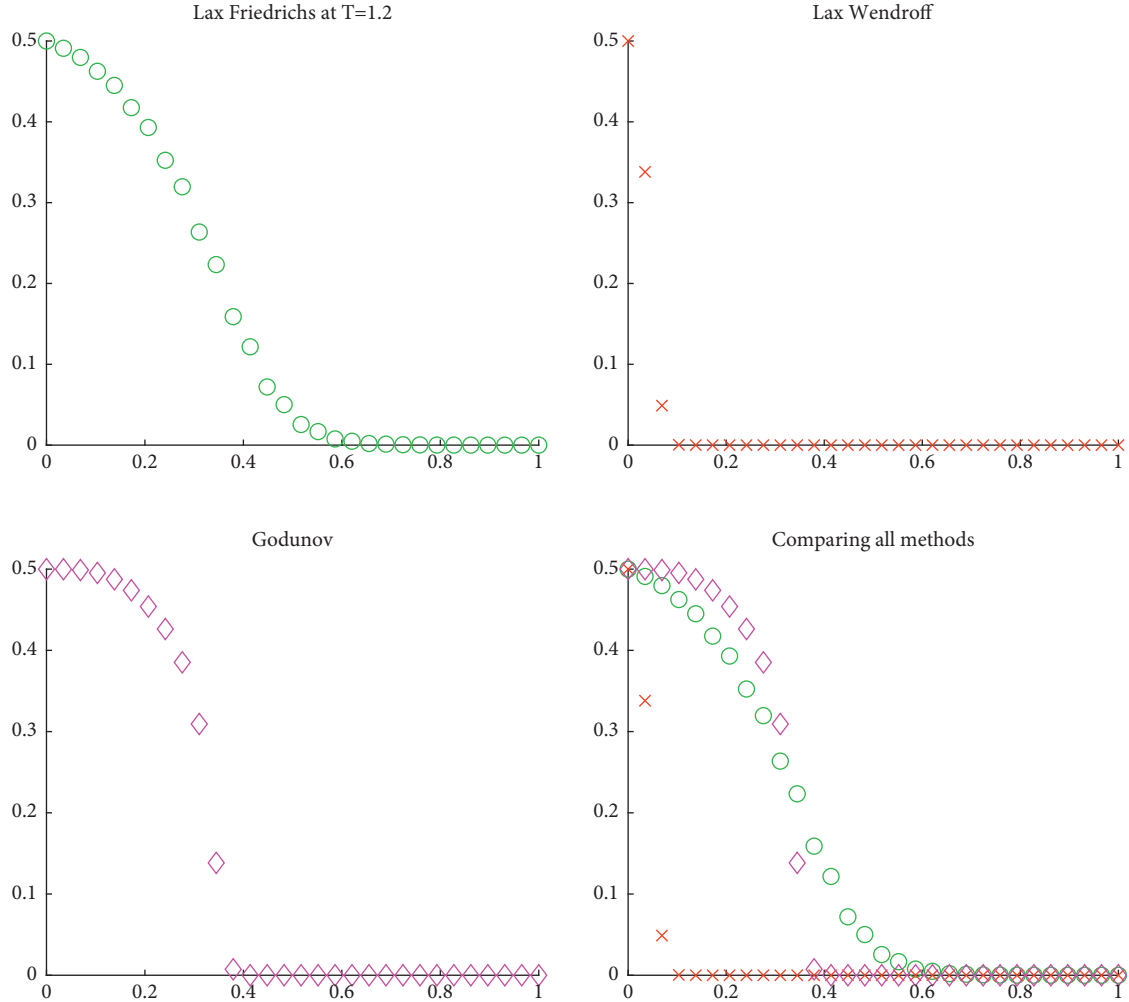


FIGURE 9: Graphs for the Buckley–Leverett simulation.

4.6. *Godunov's Scheme.* To compare the previous finite difference schemes with a finite volume scheme, we choose to use Godunov's scheme. Although this method is only first-order accurate, it is the basis of other high-order finite volume schemes. To get Godunov's method, we start by letting U_j^n be a numerical solution on the n -th layer. After that, we need to define a function $\tilde{U}^n(x, t)$ for the time interval $t_n < t < t_{n+1}$. At $t = t_n$, we have the following:

$$\begin{aligned} \tilde{U}^n(x, t) &= U_j^n, \\ x_j - \frac{h}{2} < x < x_j + \frac{h}{2}, \quad \text{for } j = 2, \dots, n-1. \end{aligned} \quad (23)$$

We also need to define $\tilde{U}(x, t)$ to be the solution of the collection of Riemann problems on that interval. Then, the solution to the next value, U_j^{n+1} , is simply defined by averaging $\tilde{U}(x, t_{n+1})$ over the interval $x_j - (h/2) < x < x_j + (h/2)$. When everything is said and done, this idea reduces to the following:

$$U_j^{n+1} = U_j^n - \frac{k}{h} [F(U_j^n, U_{j+1}^n) - F(U_{j-1}^n, U_j^n)]. \quad (24)$$

When we apply this to the Burgers equation, the numerical flux F is

$$F(U, V) = \frac{(u^*)^2}{2}, \quad (25)$$

and when we apply this to the Buckley–Leverett equation,

$$F(U, V) = \frac{(u^*)^2}{(u^*)^2 + 1/4(1 - u^*)^2}, \quad (26)$$

where u^* is defined as follows.

If $U \geq V$, then

$$u^* = \begin{cases} U, & \frac{U+V}{2} > 0, \\ V, & \text{else.} \end{cases} \quad (27)$$

If $U < V$, then

$$u^* = \begin{cases} U, & U > 0, \\ V, & V < 0, \\ 0, & U \leq 0 \leq V. \end{cases} \quad (28)$$

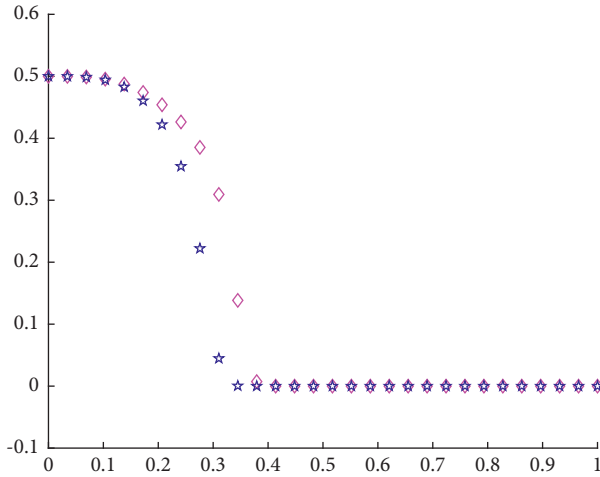


FIGURE 10: Comparing Godunov and upwind methods.

5. Results

In this section, several simulations for the Burgers equation and one simulation for the Buckley–Leverett equation are carried out. After we ran each simulation, we compared the results from the finite difference methods and the finite volume method.

5.1. Simulation 1: Single Shock. The equation and the solutions of the single shock simulation are given by equation (29) and shown in Figure 6 using the methods mentioned in Section 4.

$$u(x, 0) = \begin{cases} 1, & x < 0.1, \\ 0, & x > 0.1. \end{cases} \quad (29)$$

To satisfy the stability condition for the finite schemes, we used $h = (1/60)$ and $k = 0.005$.

We can see from the results that the finite difference methods had issues at the sharp turns (the derivative does not exist). Notice that the Lax–Friedrichs method shows diffusion at the corners while the Lax–Wendroff method produces oscillations. The Godunov method handles the shock much better, but still it is not accurate. In fact, we also wanted to point out that for the Burgers equation, the classical upwind scheme and the Godunov scheme produce the same result (see Figure 7). This is basically because $f'(u) > 0$.

5.2. Simulation 2: Traveling Pulse. The equation and the solutions of the traveling pulse simulation are given by equation (30) and shown in Figure 8 using the methods mentioned in Section 4.

$$u(x, 0) = \begin{cases} 0, & x < -1, \\ \frac{1}{2}, & -1 < x < 0, \\ 0, & x > 0. \end{cases} \quad (30)$$

In the simulation above, we used a smaller h value so that we could better see what happens at the corners; $h = 0.025$ and $k = 0.01$. We obtain the same results that we saw before with the single shock. It is interesting to note that the Lax–Wendroff method does not have oscillations at the top left corner ($x = 0$), but it does have oscillations at the other places where the derivative does not exist. Note that we did not include the upwind scheme because we knew that it would produce the same results as the Godunov scheme.

5.3. Simulation 3: Buckley–Leverett Equations. The equation and the solutions of Buckley–Leverett simulation are given by equation (31) and shown in Figure 9 using the methods mentioned in Section 4.

$$u(x, 0) = \begin{cases} \frac{1}{2}, & x = 0, \\ 0, & x > 0. \end{cases} \quad (31)$$

This produced the same results that we saw in the Burgers equation simulations. The Lax–Wendroff method does not have an oscillation by itself, but it definitely has its issues. To see the difference between the Godunov scheme and the upwind scheme, we had to use a different flux (the Buckley–Leverett flux) as shown in Figure 10.

6. Conclusion

Although we used the conservation equations to explain and illustrate the finite volume method, it can be used on any type of differential equation. We choose the conservation equations since usually finite volume methods are used on fluid flow, which is conservative. We can conclude by our comparison that the main difference of these methods can be seen in the way of approaching the solutions, as starting with a variational formulation of the problem, the finite element technique provides piecewise formulations of functions defined by a collection of grid data points, while the finite difference technique begins with a differential formulation of the problem and continues to discretize the derivatives. Moreover, the finite volume method even with the simplifications that we gave produced very good results for the simulations. In fact, it did not appear to have any difficulty handling the shocks and discontinuous derivatives, which is why FVMs are used in modelling fluid flow.

Data Availability

No data were used to support this study.

Conflicts of Interest

The authors declare that they have no conflicts of interest.

Acknowledgments

The sixth author received financial support from Taif University Researches Supporting Project number (TURSP-2020/031), Taif University, Taif, Saudi Arabia.

References

- [1] M. M. Khader, "Numerical treatment for solving fractional Riccati differential equation," *Journal of the Egyptian Mathematical Society*, vol. 21, no. 1, pp. 32–37, 2013.
- [2] G. G. Botte, J. A. Ritter, and R. E. White, "Comparison of finite difference and control volume methods for solving differential equations," *Computers & Chemical Engineering*, vol. 24, no. 12, pp. 2633–2654, 2000.
- [3] R. Eymard, T. Gallouët, and R. Herbin, "Finite volume methods," *Handbook of Numerical Analysis*, vol. 7, pp. 713–1018, 2000.
- [4] A. Chambolle and T. Pock, "Approximating the total variation with finite differences or finite elements," in *Geometric Partial Differential Equations - Part II*, vol. 22, pp. 383–417, Elsevier, Amsterdam, Netherlands, 2021.
- [5] S. Tian, X. Liu, and An Ran, "A higher-order finite difference scheme for singularly perturbed parabolic problem," *Mathematical Problems in Engineering*, vol. 2021, Article ID 9941692, 11 pages, 2021.
- [6] V. N. Kaliakin, *Introduction to Approximate Solution Techniques, Numerical Modeling, and Finite Element Methods*, CRC Press, Boca Raton, FL, USA, 2018.
- [7] S. B. G. Karakoç, A. Başhan, and T. Geyikli, "Two different methods for numerical solution of the modified Burgers' equation," *The Scientific World Journal*, vol. 2014, Article ID 780269, 13 pages, 2014.
- [8] S. Mazumder, *Numerical Methods for Partial Differential Equations: Finite Difference and Finite Volume Methods*, Academic Press, Cambridge, MA, USA, 2015.
- [9] Y. S. Younis, A. Hasan Ali, O. Kh Alhafidhb et al., "Early diagnosis of breast cancer using image processing techniques," *Journal of Nanomaterials*, vol. 2022, Article ID 2641239, 6 pages, 2022.
- [10] R. Kaur, S. Kumar, and V. K. Kukreja, "Numerical approximation of generalized burger's-Fisher and generalized burger's-huxley equation by compact finite difference method," *Advances in Mathematical Physics*, vol. 2021, Article ID 3346387, 17 pages, 2021.
- [11] H. T. Basha, K. Rajagopal, N. A. Ahammad, S. Sathish, and S. R. Gunakala, "Finite difference computation of Au-Cu/Magneto-Bio-Hybrid nanofluid flow in an inclined uneven stenosis artery," *Complexity*, vol. 2022, Article ID 2078372, 18 pages, 2022.
- [12] C. M. Okubo, L. F. N. Sá, C. Y. Kiyono, and E. C. N. Silva, "A discrete adjoint approach based on finite differences applied to topology optimization of flow problems," *Computer Methods in Applied Mechanics and Engineering*, vol. 389, Article ID 114406, 2022.
- [13] J. Weickert, "Applications of nonlinear diffusion in image processing and computer vision," *Acta Mathematica Universitatis Comenianae. New Series*, vol. 70, 2000.
- [14] A. M. Ghazi, A. Ali Hasan, Al-G. Khalil S, A. Jan, and B. Omar, "Nonlinear stability and linear instability of double-diffusive convection in a rotating with LTNE effects and symmetric properties: brinkmann-forchheimer model," *Symmetry*, vol. 14, no. 3, p. 565, 2022.
- [15] S. W. Key and R. D. Krieg, "Comparison of finite-element and finite-difference Methods* * This work was supported by the United States atomic energy commission," in *Numerical and Computer Methods in Structural Mechanics*, pp. 337–352, Academic Press, Cambridge, MA, USA, 1973.
- [16] O. C. Zienkiewicz, R. L. Taylor, and R. L. Taylor, *The Finite Element Method: Solid Mechanics*, Vol. 2, Butterworth-Heinemann, Oxford, UK, 2000.
- [17] E. Oñate, *Structural Analysis with the Finite Element Method. Linear Statics: Volume 2: Beams, Plates and Shells*, Springer Science & Business Media, New York, NY, USA, 2013.
- [18] M. Karahan, O. Kalenderli, and V. Vikhrenko, "Coupled electrical and thermal analysis of power cables using finite element method," *Heat Transfer-Engineering Applications*, vol. 205, 2011.
- [19] B. Almarri, A. H. Ali, K. S. Al-Ghafri, A. Almutairi, O. Bazighifan, and J. Awrejcewicz, "Symmetric and non-oscillatory characteristics of the neutral differential equations solutions related to p-laplacian operators," *Symmetry*, vol. 14, no. 3, p. 566, 2022.
- [20] B. Almarri, A. H. Ali, A. M. Lopes, and O. Bazighifan, "Nonlinear differential equations with distributed delay: some new oscillatory solutions," *Mathematics*, vol. 10, no. 6, p. 995, 2022.
- [21] W. Ibrahim and G. Gadisa, "Finite element method solution of boundary layer flow of powell-eyring nanofluid over a nonlinear stretching surface," *Journal of Applied Mathematics*, vol. 2019, Article ID 3472518, 16 pages, 2019.